Supplemental Information.

Effects of peptides derived from terminal modifications of the Aβ central hydrophobic core on Aβ fibrillization

Cyrus K. Bett,[1] Wilson K. Serem,[1] Krystal R. Fontenot,[1] Robert P. Hammer[2] and Jayne C. Garno[1]*

[1]Department of Chemistry, Louisiana State University, Baton Rouge, LA 70803

[2]New England Peptide LLC, 65 Zub Lane, Gardner, MA 01440
Phone: 978-630-0020 E-mail: rphammer@gmail.com

*corresponding author: Jayne C. Garno
Phone: 225-578-8942
E-mail: jgarno@lsu.edu

*address Chemistry Department
Louisiana State University
232 Choppin Hall
Baton Rouge, LA 70803

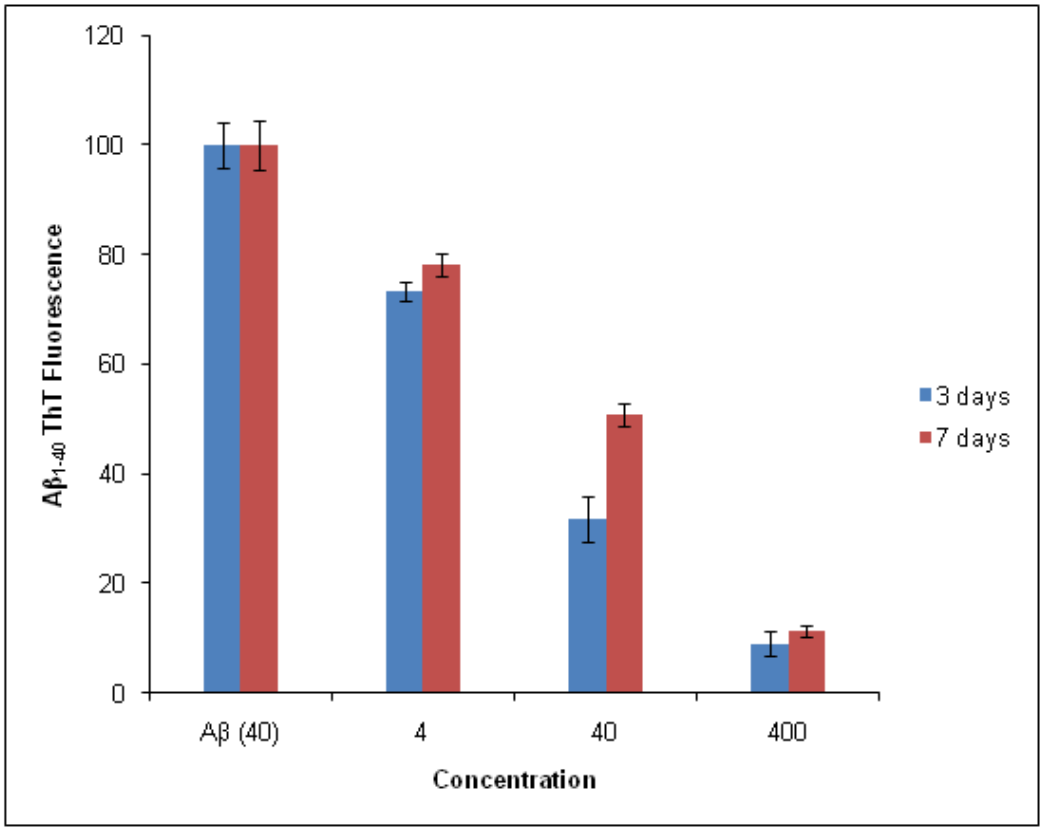

Figure S1. Concentration dependent study of the assembly of $A\beta_{1-40}$ in the presence of AAMP-14. Fluorescence (ThT) was set arbitrarily to 100 percent relative to $A\beta_{1-40}$.

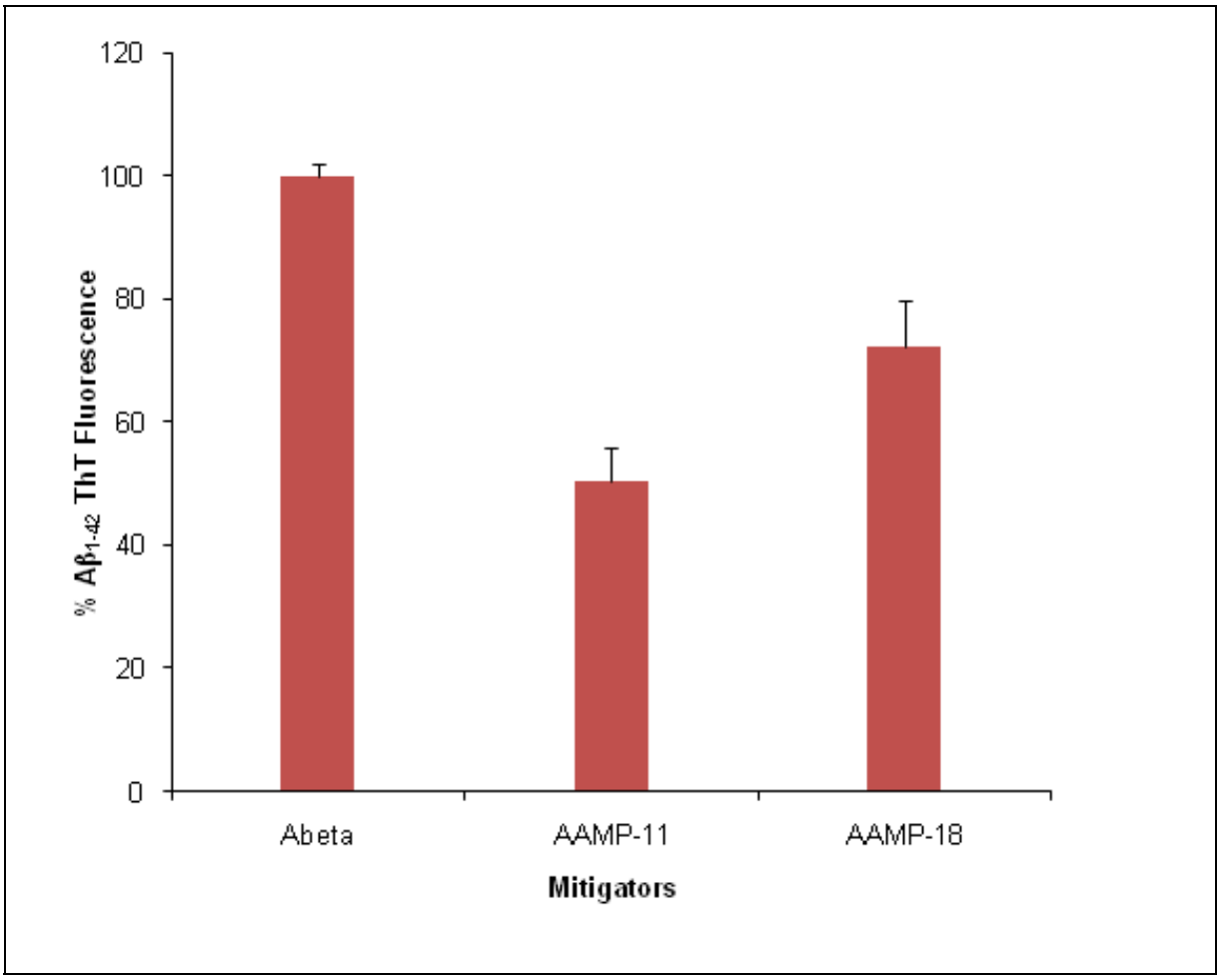

Figure S2. Assembly of $A\beta_{1\text{-}42}$ in the presence of ααAA-AAMPs. Time-dependent ThT fluorescence monitoring of $A\beta_{1–42}$ assembly in the presence or absence of the various AAMPs. Fluorescence (ThT) was set arbitrarily to 100 percent relative to $A\beta_{1–42}$.

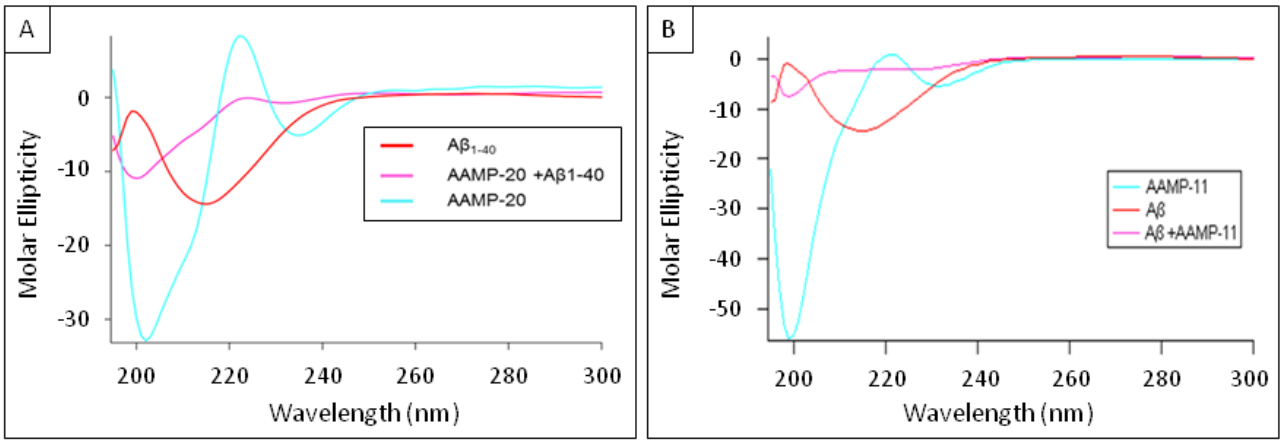

Figure S3. Example CD signatures obtained for $A\beta_{1\text{-}40}$ mitigation by [A] AAMP-20 and [B] AAMP-11 after aging samples for one week.

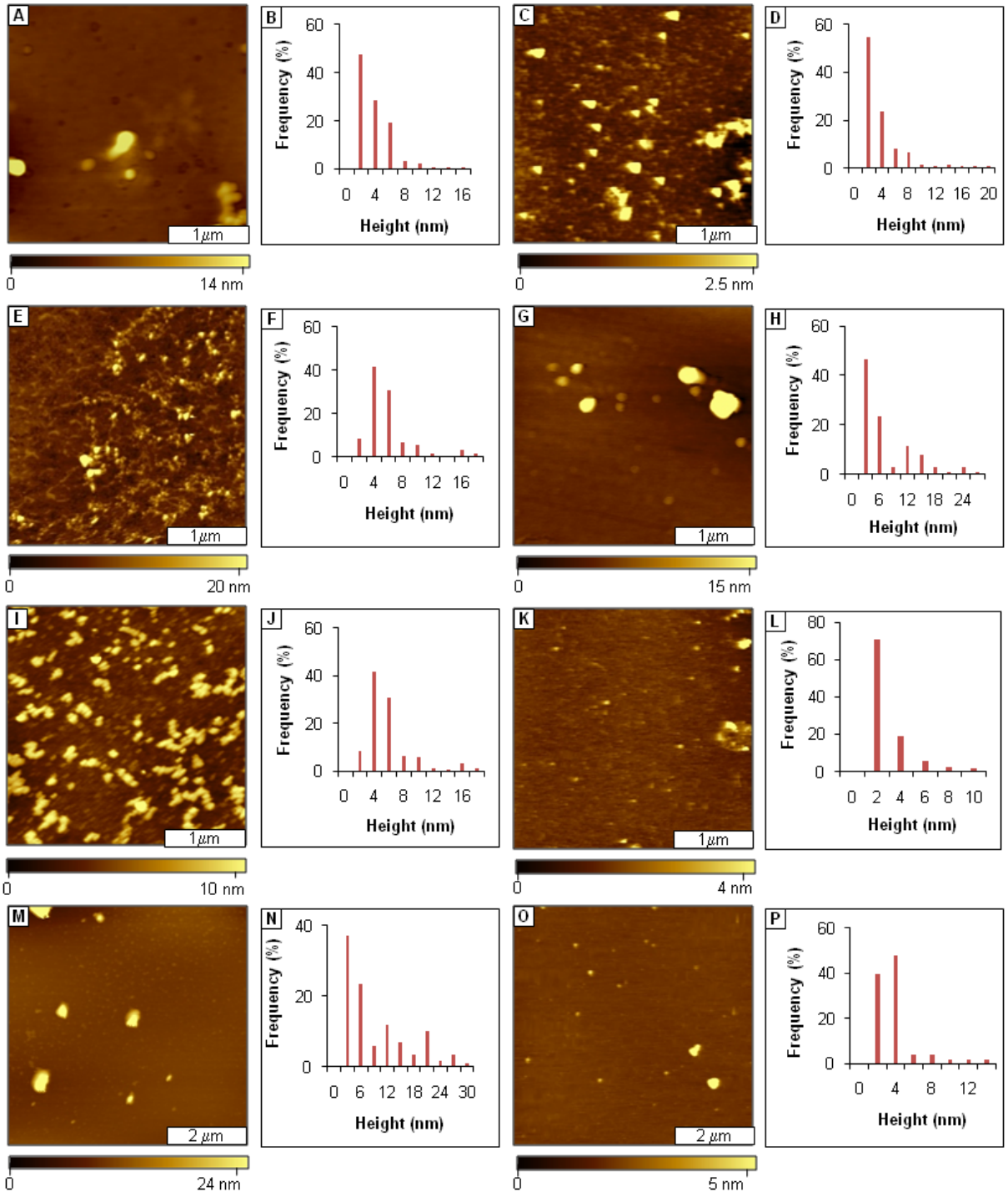

Figure S4. Spherical aggregates observed after one week of aging the various AAMPs alone. Topographic AFM views of spherical structures formed by: [A] AAMP-11 [B] corresponding height analysis for A; [C] AAMP-12 [D] height analysis for C; [E] AAMP-13; [F] height analysis for E; [G] AAMP-14; [H] height histogram for G; [I] AAMP-15; [J] height analysis for I; [K] AAMP-16; [L] height histogram for K; [M] AAMP-17; [N] height analysis for M; [O]AAMP-18; [P] height distribution for O; [Q]AAMP-19; [P] height analysis for Q.

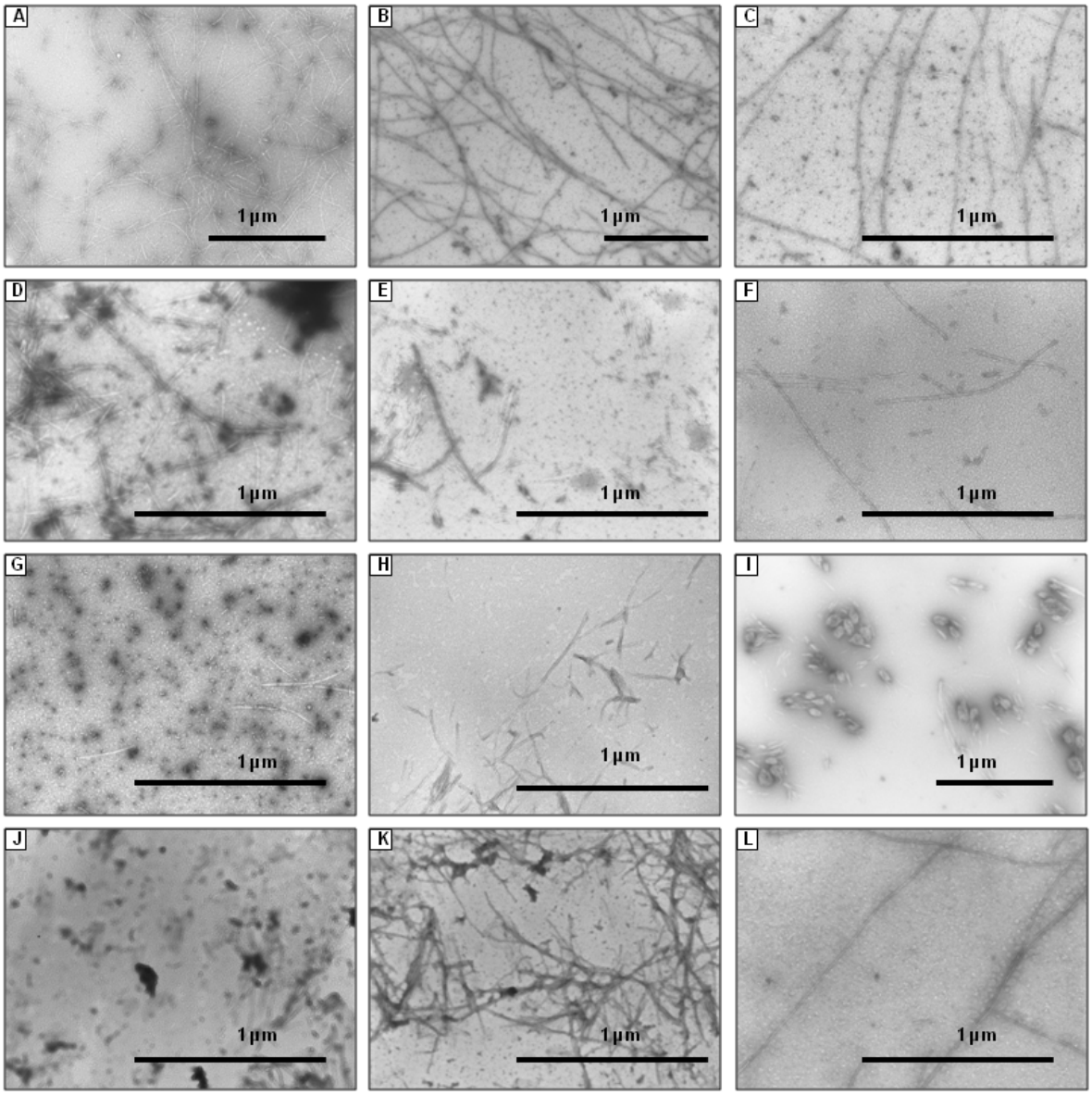

Figure S5 (A). Morphologies of various surface structures observed after one week of aging $A\beta_{1\text{-}40}$ in the presence of various AAMPs with no ααAAs observed with TEM micrographs. [A] Fibrils formed by $A\beta_{1\text{-}40}$ alone; [B] fibrils formed by $A\beta_{1\text{-}40}$ alone, different view; [C] fibrils formed by $A\beta_{1\text{-}40}$ alone, zoom in view of sample B; [D] fibrils formed from $A\beta_{1\text{-}40}$ mitigation by AAMP-11; [E] spherical particles and fibrils formed from aging $A\beta_{1\text{-}40}$ in the presence of AAMP-12; [F] spherical particles and isolated fibrils were observed from aging a mixture of $A\beta_{1\text{-}40}$ and AAMP-13; [G] spherical particles formed from mitigation of $A\beta_{1\text{-}40}$ aggregation by AAMP-14; [H] Mixture of spherical aggregates and short fibrils were observed from incubating $A\beta_{1\text{-}40}$ in the presence of AAMP-15; [I] spherical particles formed from mitigation of $A\beta_{1\text{-}40}$ aggregation by AAMP-16 [J] spherical aggregates observed from mitigation of $A\beta_{1\text{-}40}$ aggregation by AAMP-17; [K] fibrils formed from $A\beta_{1\text{-}40}$ mitigation by AAMP-18; [L] fibrils formed from $A\beta_{1\text{-}40}$ mitigation by AAMP-19.

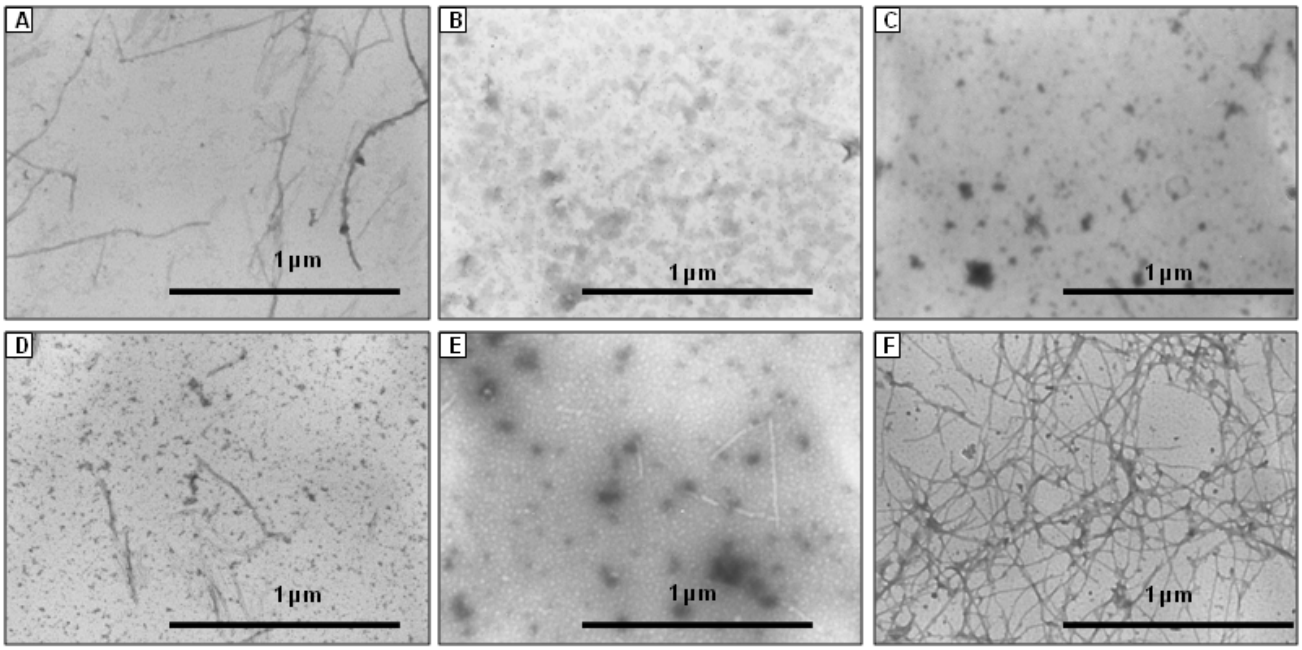

Figure S5 (B). Morphologies of various surface structures observed after one week of aging $A\beta_{1\text{-}40}$ in the presence of various AAMPs with ααAAs, observed with TEM micrographs. [A] Fibrils formed from mitigation of $A\beta_{1\text{-}40}$ by AAMP-20; [B] spherical particles formed from aging $A\beta_{1\text{-}40}$ in the presence of AAMP-21; [C] spherical particles were observed from aging a mixture of $A\beta_{1\text{-}40}$ and AAMP-22; [D] spherical particles and isolated fibrils formed from mitigation of $A\beta_{1\text{-}40}$ aggregation by AAMP-23; [E] mixture of spherical aggregates and short fibrils were observed from incubating $A\beta_{1\text{-}40}$ in the presence of AAMP-24; [F] fibrils formed from mitigation of $A\beta_{1\text{-}40}$ by AAMP-25